

# Silibinin Inhibits the Hepatocellular Carcinoma in NDEA-Induced Rodent Carcinogenesis Model: An Evaluation through Biochemical and Bio-Structural Parameters

Abhishek Kumar<sup>1</sup>, Priyashree Sunita<sup>2,3</sup> and Shakti P Pattanayak<sup>1,3\*</sup>

<sup>1</sup>Division of Pharmacology, Department of Pharmaceutical Technology and Sciences, Birla Institute of Technology, Mesra, Ranchi- 835215, India

<sup>2</sup>Government Pharmacy Institute, Department of Health Education and Family Welfare, Govt. of Jharkhand, Bariatu-834009, Ranchi, Jharkhand, India

<sup>3</sup>Department of Pharmacology, School of Pharmacy - Faculty of Medicine, The Hebrew University of Jerusalem, Jerusalem- 91120, Israel

## Abstract

The present study was aimed to investigate the chemopreventive potential of Silibinin (SIB) against N-nitrosodiethylamine (NDEA)-induced hepatocellular carcinoma (HCC) in wistar rats. Thirty experimental animals were subjected to partial hepatectomy (PH) and after 24 hours of stabilization period a single dose of NDEA (100 mg/kg b.w., i.p) was administered to each animal followed by CCl<sub>4</sub> (1 ml/kg b.w., s.c.). The effect of SIB (25 and 50 mg/kg/day, i.p.) on NDEA-induced HCC was determined after 2 weeks of treatment (6<sup>th</sup> to 8<sup>th</sup> week after PH, in the promotional stage of tumor development). NDEA treatment to rats resulted in significant decrease in body weight and increase in liver weight along with levels of transaminases,  $\gamma$ -glutamyl transferase, lipoprotein, glycoproteins. Hepatic and serum malondialdehyde content, enzymatic and non-enzymatic antioxidant levels were also altered in HCC bearing animals without treatment. Bio-structural components (such as amide bands of proteins, symmetric phosphate stretching of nucleic acids, methylene chains in membrane lipids, methyl to methylene ratio of carbohydrates and proteins etc.) were marked in NDEA-treated groups of animals by analysing changes in the position and intensities of the peaks in Fourier transform infrared spectroscopy (FTIR). Immunohistochemical staining of Ki67 and histopathological analysis were also carried out in order to support the study. SIB treatment could attenuate NDEA-induced hepatocarcinogenesis by improving the biochemical and bio-structural changes of the hepatic tissue near normal levels in a dose dependent manner. Taken together, this study reveals that SIB may have potential as a multi-functional drug candidate for cancer therapy.

**Keywords:** Liver cancer; NDEA; Silibinin; Biochemical; Bio-structural; FTIR

## Introduction

Liver cancer is one of the most common malignancies worldwide, especially in Asia and Africa [1]. Hepatocellular carcinoma (HCC) accounts for about 80-90% of all cancers and ranks the fifth most common and the third most deadly cancer worldwide [2]. Major risk factors for liver cancer include hepatitis viral infection, food additives, alcohol, aflatoxins, industrial toxic chemicals air and water pollutants, etc. [3].

N-nitrosodiethylamine (NDEA), is a well-known potent hepatocarcinogenic agent present in tobacco smoke, water, cured and fried meals, cheddar cheese, agricultural chemicals, cosmetics and pharmaceutical products [4]. It is an important environmental carcinogen produces reproducible tumor in the liver [5]. Administration of NDEA has been reported to generate lipid peroxidation and activate oxygen species during hepatocarcinogenesis [6]. Oxidative stress has recently been suggested to participate in both metabolism and carcinogenic actions of nitrosamine. Liver tumor promotion in rodents has been characterized most extensively in the rat model utilizing initiation with a nitrosamine, partial hepatectomy (PH), and subsequent promotion with polychlorinated aromatic hydrocarbons [7]. The possibility was raised that the tumor yield in the liver would be increased, if NDEA were given in the period of regeneration that followed a necrotizing dose of a hepatotoxin like CCl<sub>4</sub> that was not full carcinogen by itself [8]. Taken together the use of NDEA for HCC animal model development is a potential tool which mimics the HCC in clinical findings.

Recent approach of chemoprevention serves as an attractive alternative to control malignancy. Flavonoids have been shown to act

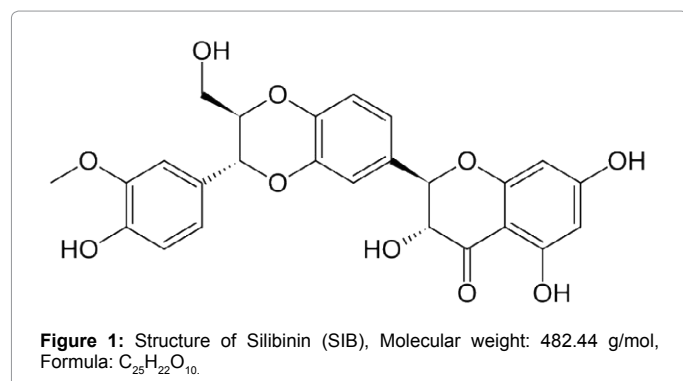
as scavengers of various oxidizing species, inhibit the growth of various cancer cell lines *in vitro*, and reduce tumor development in experimental animals [9,10]. Milk thistle (*Silybum marianum*) is the most ancient and extensively used medicinal plant for its beneficial effects on liver and other organs [11]. Silymarin, an extract isolated from its fruits and seeds, is known to provide a wide range of hepatoprotective effects, especially against diseases like hepatitis, cirrhosis and jaundice [12]. Marketed as Legalon or Flavobion, silymarin has been successfully applied in the therapy of various liver diseases. Moreover, highly efficient antitumour activities were also reported for Silymarin [13,14]. One of the most active constituents is Silibinin (SIB) [(2R,3R)-3,5,7-trihydroxy-2-[(2R\*,3R\*)-3-(4-hydroxy-3-methoxyphenyl)-2-hydroxymethyl-1,4-benzodioxane-6-yl]-4-chromanone], which is composed of flavanone-3-ol and 1,4-benzodioxane ring systems (Figure 1). Silibinin, is consumed widely as a dietary supplement and it displays a remarkable spectrum of pharmacological activities like antioxidant, hepatoprotective, anti-inflammatory, antibacterial, antiallergic, antimutagenic, antiviral, antineoplastic, antithrombotic

**\*Corresponding author:** Shakti P. Pattanayak, Department of Pharmacology, School of Pharmacy - Faculty of Medicine, The Hebrew University of Jerusalem, Jerusalem-91120, Israel Tel: +972-58-6243563/67; E-mail: [sppattanayak@bitmesra.ac.in](mailto:sppattanayak@bitmesra.ac.in); [shakti.pattanayak@mail.huji.ac.il](mailto:shakti.pattanayak@mail.huji.ac.il)

Received April 15, 2015; Accepted July 13, 2015; Published July 16, 2015

**Citation:** Kumar A, Sunita P, Pattanayak SP (2015) Silibinin Inhibits the Hepatocellular Carcinoma in NDEA-Induced Rodent Carcinogenesis Model: An Evaluation through Biochemical and Bio-Structural Parameters. J Cancer Sci Ther 7: 207-216. doi:10.4172/1948-5956.1000352

**Copyright:** © 2015 Kumar A, et al. This is an open-access article distributed under the terms of the Creative Commons Attribution License, which permits unrestricted use, distribution, and reproduction in any medium, provided the original author and source are credited.



and vasodilatory actions [15,16], affecting basic cell functions such as proliferation, differentiation and apoptosis. It possesses anticancer effect on human hepatocellular carcinoma cells [17] and also it produced antitumor efficacy in an orthotopic drafting of Hep-55.1C cells into the liver of C57BL/6 mice [18]. Based on these claim, we for the first time tried to evaluate the effect of SIB on NDEA-induced hepatocellular carcinogenesis model which represents all stages of carcinogenesis *in vivo* (Figure 2).

## Materials and Methods

### Animals

Wistar albino rats 50-day old were purchased from National Institute of Nutrition, Hyderabad, India and used for the study. Animals were maintained on standard pelleted diet and water *ad libitum*. Experiments were approved by the Animal Ethics Committees of Department of Pharmaceutical Technology and Sciences, Birla Institute of Technology University, India (621/02/ac/CPCSEA) and strictly performed according to the NIH and CPCSEA, India guidelines for the care and use of laboratory animals.

### Chemicals

N-Nitrosodiethylamine was obtained from the Sigma Aldrich, USA. KBr (I.R. Grade), Silibinin (M.W.: 482.44g/mol) and other fine chemicals were purchased from the Sigma Aldrich, USA. Other chemicals and reagents in the study are of highest purity and standard which are commercially available.

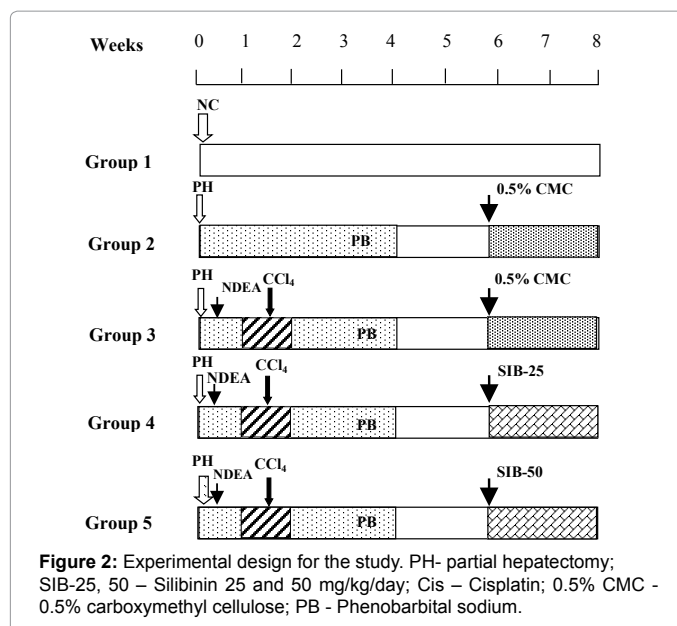
### Tumor induction and experimental design

HCC was induced by NDEA using the induction techniques given by Yadav et al. [5], Pound et al. [8] with some modifications. Briefly, PH was done to the animals. After 24 hours of stabilization a single dose of NDEA (100 mg/kg b.w., i.p) was administered to the animals. Phenobarbital sodium (PB, 0.05% w/v, P.O.) was given after PH, up to 4 weeks in drinking water. CCl<sub>4</sub> (1 ml/kg b.w., s.c.) was administered twice a week from 1<sup>st</sup> week to 2<sup>nd</sup> week.

Tumor yield and size were stabilized after 6 weeks with the initiation of NDEA. The administration of SIB was done after 6 weeks of NDEA-treatment and continued up to 8 weeks (in the promotional stage of tumor development). Five experimental groups with six animals in each group were set up in this study as follows:

Group I: Animals with no treatment

Group II: PH was performed to the animals and received only 0.5% CMC (Vehicle)



Group III: HCC induced with NDEA (200 mg/kg b.w., i.p.) as described (after 24h stabilization of PH) and received only 0.5% CMC for the treatment period

Group IV: Animals with HCC were treated with SIB-25 (after 6 weeks)

Group V: Animals with HCC were treated with SIB-50 (after 6 weeks)

The animals in each group were weighted each week and the changes in the body weight were recorded. All the animals were starved overnight and sacrificed by cervical decapitation after the completion of 8th week.

### Macroscopical documentation of tumor burden and sample preparation

After decapitation of the animals in each group, the livers were isolated and cleaned properly using phosphate buffer saline (PBS), weighted and observed morphologically for: foci, lesions and tumors. Blood was collected; the plasma and serum were separated by centrifugation. Liver specimens were cleared for surrounding fat, weighed and cut into small pieces. 1g of tissue sample was isolated from liver and freeze dried for infrared spectroscopy sampling. The other part of the liver was washed with ice cold normal phosphate buffer saline (PBS), pH 7.2 and cut into small pieces with a heavy duty blade. Tissues were homogenized by glass homogenizer tube in cold PBS, centrifuged at 20,000 rpm for 10 min. The tissue homogenate and serum were used for the estimation of biochemical parameters.

### Biochemical estimations

Aspartate dehydrogenase (AST) and alanine transaminase (ALT) were estimated in serum and homogenate by the method of King, 1965 with some modifications [19,20]. Alkaline phosphatase (ALP) was estimated according to the modified method of Belfield and Goldberg et al. [21] and gamma glutamyl transferase (GGT) by the standard method in both serum and homogenate as well [22]. Lipid peroxidation (LPO) was measured by the method of Ohkawa et al. [23]. LPO was expressed as nanomoles of malondialdehyde (MDA) formed by using

an extinction coefficient of  $0.152 \text{ mM}^{-1} \text{ cm}^{-1}$  formed per milligram of protein. The protein content was estimated by the method of Lowry et al. [24]. Superoxide dismutase (SOD) activity was assessed by the nitroblue tetrazolium reduction method by Flohe and Otting et al. [25]. Catalase (CAT) activity was assayed by the method of Sinha [26] and ascorbic acid and  $\alpha$ -tocopherol were also accessed [20]. Oxidation of glutathione by the enzyme was measured spectrophotometrically at 420 nm. The activity of GPx was expressed as micromoles glutathione oxidized per minute per milligram protein by Rotruck et al. [27]. Reduced glutathione (GSH), Glutathione reductase (GR) was estimated by the method of Moron et al. and glutathione-S-transferase (GST) [28].

The lipids in plasma was extracted and quantified by the method of Folch et al. [29]. Triglyceride was estimated using the method of Rice et al. [30], which is based on the method of Van Handle et al. [31]. Total cholesterol was estimated using the method of Parekh and Jung et al. [32]. Plasma lipoproteins were fractionated by dual precipitation technique of Sujatha and Sachdanandam et al. [33]. Addition of heparin-magnesium to plasma, precipitated very low-density lipoproteins (VLDL-c), low-density lipoproteins (LDL-c), and high-density lipoproteins (HDL-c), which were left in the supernatant, and subsequently, the content was measured in the fraction. The protein bound hexose, protein bound hexosamine and protein bound sialic acid was estimated from the collected serum samples by the method of Nandave et al. [34].

### Histopathological and immunohistochemical studies

For histopathological examination, liver tissues specimens from all groups were fixed in 10% neutral-buffered formalin. The histopathology of the tissue samples with Hematoxylin and eosin staining were carried out by the modified method of Pattanayak et al. [35]. To the paraffin sections of the liver tissue, Ki67 immunolabeling was performed to assess cell proliferation [36], using a mouse monoclonal antibody (Thermo Scientific, USA), and a three-step immunoperoxidase method.

### FT-IR spectroscopic analysis

The FT-IR spectra in the  $4000\text{--}400\text{cm}^{-1}$  region were recorded with a Shimadzu 8400S FT-IR Spectrometer equipped with an attenuated reflectance detector (ATR) detector. FTIR analysis was done according to the method of Palaniappan et al. [37] with some modifications. In brief, 3 mg lyophilized sample was triturated with 100 mg IR grade KBr and pelleted for standard FT-IR analysis. The spectrometer was continuously purged with dry nitrogen to eliminate atmospheric water vapor and carbon dioxide. To improve the signal to noise ratio for each spectrum, 60 scans with a spectral resolution of  $\pm 4 \text{ cm}^{-1}$  were averaged. Background spectra, which were collected under identical conditions, were subtracted from the sample spectra automatically. The frequencies for all sharp bands were accurate to  $0.001 \text{ cm}^{-1}$ . To eliminate the differences due to the non-uniformity of thickness of sample and the varying of intensity of light source, all spectra were subsequently calibrated. The frequencies for all sharp bands were determined accurately from the original base line-corrected spectra belonging to the corresponding four groups. Each observation was confirmed by taking at least three replicates. The sample was then weighed to get the quantitative data. Therefore, it was possible to directly correlate the intensities of absorption bands to the concentration of the functional group. The spectra were analyzed using Shimadzu IRsolution software.

### Statistical analysis

Pharmacological data were analyzed by one-way analysis of variance followed by Bonferroni's multiple comparison tests with equal sample

size. The difference was considered significant when  $p$  value  $<0.05$ . All the values were expressed as mean  $\pm$  standard error mean (SEM).

## Results

### SIB ameliorated the alteration in body weight and liver weight in NDEA-induced liver cancer

NDEA treatment caused significant difference in body weight (b.w.) as compared with normal control and PH-control groups. SIB treatment in NDEA treated animals showed significant increase ( $p < 0.001$ ) in b.w. with respect to induced control in both treatment groups (Figure 3). NDEA treatment caused highly significant ( $p < 0.001$ ) increase in liver weight. SIB (25 mg/kg/day) administration caused significant ( $p < 0.05$ ) decrease and higher dose (SIB-50 mg/kg/day) caused complete normalization of liver weight (Figure 4). The representative images of the liver of all groups of rats are depicted in Figure 5.

### Antioxidant status and biochemical changes in HCC-rats were attenuated by SIB

NDEA treated rats showed significant ( $p < 0.01$ ) increase in the AST, ALT, ALP and  $\gamma$ -GT levels in the serum (Figure 6) and tissue homogenate (Figure 7) as compared to the control group animals. SIB treatment produced significant ( $p < 0.05$ ) decrease in the liver marker levels in both treatment groups of animals. High dose treated animals showed more significant ( $p < 0.01$ ) decrease in the transaminase and  $\gamma$ -GT enzymes with respect to induced control group.

Table 1 represents the plasma lipoprotein cholesterol profile such as HDL-c, LDL-c, and VLDL-c levels of all groups along with TC and TG. The levels of HDL-c significantly ( $p < 0.001$ ) decreased in group III animals as compared with those in group I. The levels of VLDL-c and LDL-c significantly ( $p < 0.001$ ) increased in the same manner. However, significantly ( $p < 0.05$ ) decreased levels of VLDL-c, LDL-c and increased levels of HDL-c were observed in groups IV, and V animals as compared with those in group III animals. The TC and TG levels were also found

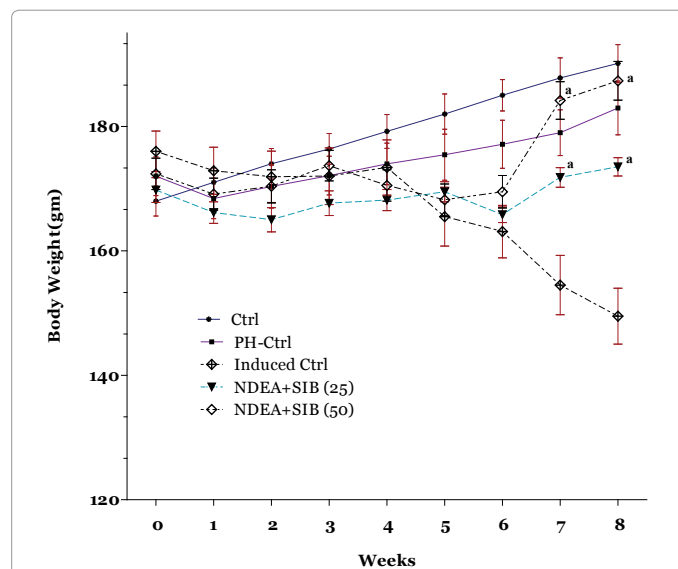
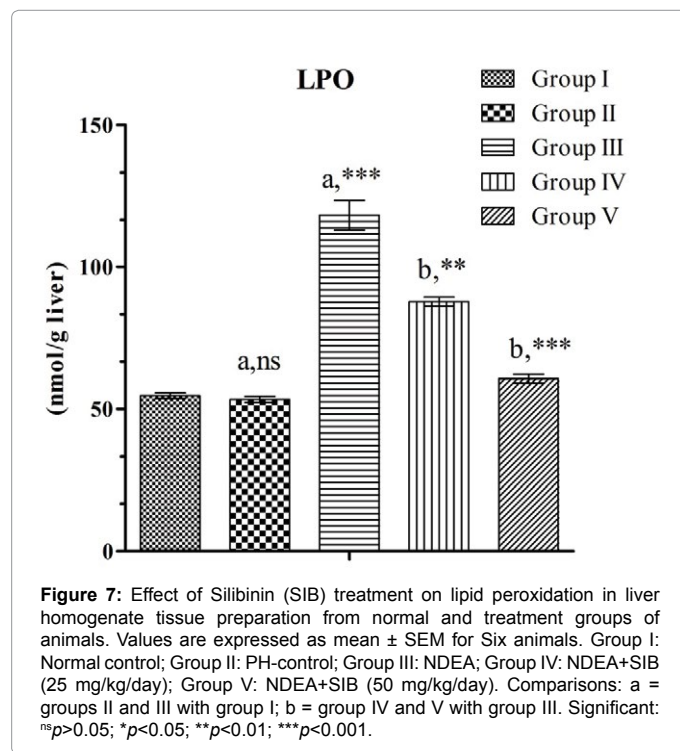
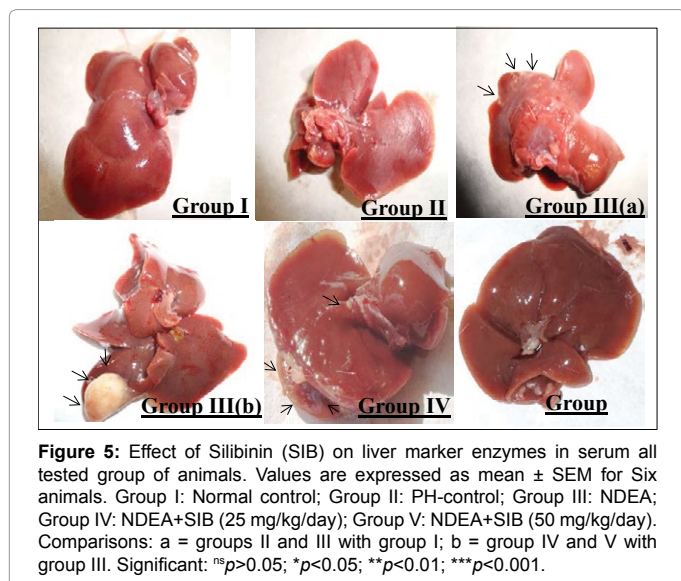
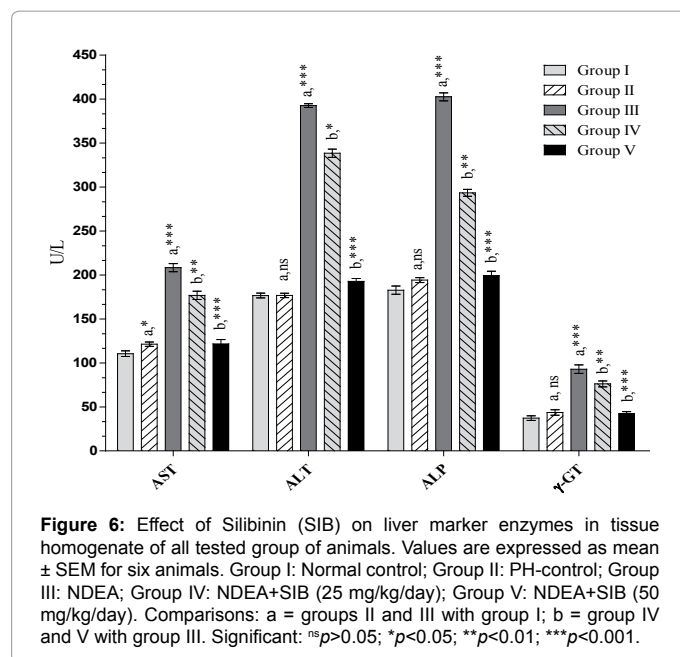
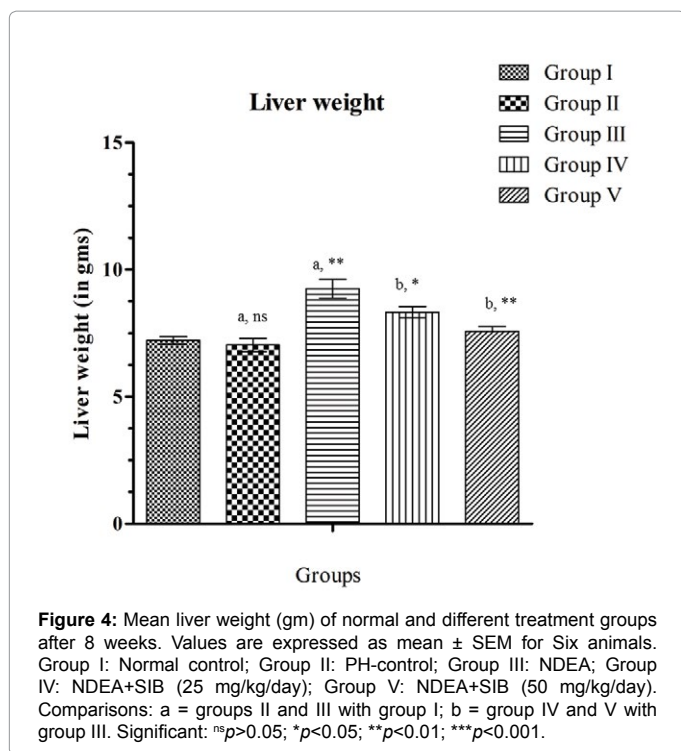


**Figure 3:** Mean body weight (gms) of normal and different groups of animals for 8 weeks of experimental period. Comparisons: NDEA+SIB (25) and NDEA+SIB (50) groups of animals compared with Induced control (induced-ctrl). Values are expressed as Mean  $\pm$  standard deviations. Significant:  $a < 0.01$ .



to be significantly increased in the Group III animals and brought back to normal levels in a dose dependent manner after the SIB treatment.

Table 2 shows activities of glycoproteins in the serum in all experimental groups. A significant ( $P<0.01$ ) increase in activity of sialic acid, hexose and hexosamine were observed in the group III animals. After the treatment with SIB for 2 weeks, these alterations in glycoprotein levels significantly decreased in a concentration dependent manner (group IV and V) (Figure 8).

The activities antioxidants in serum and liver homogenates were depicted in Tables 3 and 4, respectively. The status of SOD, CAT, GSH, GR, GPx and GST were recorded to be significantly ( $p<0.001$ ) increased

in serum samples of NDEA-induced group as compared to control group I. Although the low dose SIB (25 mg/kg/day) treatment increased the antioxidant levels HCC mice, but a propound increase was observed with the high dose (50 mg/kg/day) treatment group of animals (Table 3). The similar findings were also recorded for the enzymic and non-enzymic antioxidant levels in liver tissue homogenates of all tested groups (Table 4). The levels of lid peroxidation in only NDEA-treated animals (group III) was significantly increased ( $p<0.01$ ) with respect to group I animals and it was brought back to almost normal levels after 14 day treatment with SIB at a dose level of 50 mg/kg/day.

Groups	Group I	Group II	Group III	Group IV	Group V
TC(mg/dl)	8.23 ± 0.8	8.55 ± 0.18 <sup>a, ns</sup>	18.22 ± 0.08 <sup>a,***</sup>	14.35 ± 0.14 <sup>b,*</sup>	9.32 ± 0.34 <sup>b,***</sup>
HDL-c(mg/g wet tissue)	41.65 ± 1.07	45.24 ± 0.52 <sup>a, ns</sup>	22.95 ± 0.45 <sup>a,***</sup>	30.08 ± 0.80 <sup>b,*</sup>	42.38 ± 0.06 <sup>b,***</sup>
LDL-c(mg/g wet tissue)	54.33 ± 0.44	60.50 ± 0.41 <sup>a, ns</sup>	132.28 ± 0.15 <sup>a,***</sup>	104.41 ± 0.62 <sup>b,*</sup>	69.40 ± 0.02 <sup>b,***</sup>
VLDL-c(mg/g wet tissue)	18.32 ± 0.15	19.05 ± 0.32 <sup>a, ns</sup>	53.20 ± 1.90 <sup>a,***</sup>	40.12 ± 0.14 <sup>b,**</sup>	21.12 ± 0.05 <sup>b,***</sup>
TG	93.40 ± 1.56	94.88 ± 1.01 <sup>a, ns</sup>	192.32 ± 1.57 <sup>a,***</sup>	156.71 ± 1.20 <sup>b,*</sup>	121.67 ± 1.34 <sup>b,***</sup>

Values are expressed as mean ± SEM for Six animals. Group I: Normal control; Group II: PH-control; Group III: NDEA; Group IV: NDEA+SIB(25mg/kg/day); Group V: NDEA+SIB(50mg/kg/day). Comparisons: a = groups II and III with group I; b = group IV and V with group III. Significant: <sup>ns</sup>p>0.05; <sup>\*</sup>p<0.05; <sup>\*\*</sup>p<0.01; <sup>\*\*\*</sup>p<0.001.

**Table 1:** Effect of Silibinin (SIB) on lipoprotein levels in plasma of induced and treatment groups.

Groups (mg/g)	Group I	Group II	Group III	Group IV	Group V
Hexose	30.0 ± 0.65	34.39 ± 0.71 <sup>a,*</sup>	57.32 ± 0.56 <sup>a,***</sup>	49.67 ± 0.34 <sup>b,*</sup>	38.24 ± 0.41 <sup>b,***</sup>
Hexosamine	22.16 ± 0.39	20.78 ± 0.42 <sup>a, ns</sup>	40.26 ± 0.22 <sup>a,***</sup>	32.63 ± 0.61 <sup>b,***</sup>	23.09 ± 0.30 <sup>b,***</sup>
Sialic acid	26.22 ± 0.44	26.60 ± 0.37 <sup>a, ns</sup>	45.23 ± 0.51 <sup>a,***</sup>	38.27 ± 0.57 <sup>b,*</sup>	31.26 ± 0.80 <sup>b,***</sup>

Values are expressed as mean ± SEM for Six animals. Group I: Normal control; Group II: PH-control; Group III: NDEA; Group IV: NDEA+SIB (25 mg/kg/day); Group V: NDEA+SIB (50 mg/kg/day). Comparisons: a = groups II and III with group I; b = group IV and V with group III. Significant: <sup>ns</sup>p>0.05; <sup>\*</sup>p<0.05; <sup>\*\*</sup>p<0.01; <sup>\*\*\*</sup>p<0.001.

**Table 2:** Effect of SIB on glycoprotein level in serum of induced and treatment groups of animals.

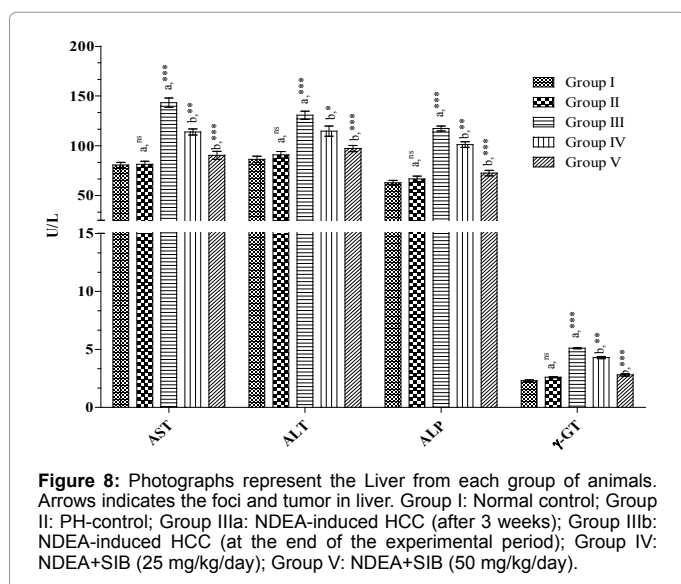


**Figure 8:** Photographs represent the Liver from each group of animals. Arrows indicates the foci and tumor in liver. Group I: Normal control; Group II: PH-control; Group IIIa: NDEA-induced HCC (after 3 weeks); Group IIIb: NDEA-induced HCC (at the end of the experimental period); Group IV: NDEA+SIB (25 mg/kg/day); Group V: NDEA+SIB (50 mg/kg/day).

### SIB-treatment customized the tissue architecture and hepatocytes proliferation in HCC

The histopathological examination of liver sections of NDEA-treated rats showed multiple nucleoli, hyperchromatic malignant nuclei, cellular infiltration, protein and cytoplasmic leakage (Figure 9) in comparison to the PH-control and normal control animals liver. A decrease in degenerative changes and cytoplasmic leakage was showed in SIB (25 mg/kg/day) and SIB (50 mg/kg/day) treated animals (Figure 9) groups. But the high dose revealed almost normal architecture comparison to the low dose treated group of animals.

The kinetics of hepatocytes proliferation was examined by Ki67-immunolabeling. A high proportion of hepatocytes were Ki67-positive (brown colored in Figure 10 (NDEA)). The rate of hepatocytes proliferation in the SB-treated animals progressively decreased thereafter (Figure 10 NDEA+SIB (25), SIB (50)). At the end of follow-up, the rate of hepatocytes proliferation had returned to basal levels in high dose treated groups of animals.

### Changes in the bio-structural components has been altered by SIB in HCC-bearing rats

A complete scanning of the normal as well as other treated group

samples was done. The general band assignments of the FTIR spectra of liver tissue on the basis of reported literature of Wistar rat for comparison among all groups were depicted in supplemental Table 1. The FT-IR spectra for the normal and PH-control group tissues (Figure 11a) showed no difference in spectral peak positions. The spectra of NDEA-induced group was compared with normal control group (Figure 11b), the spectra showed many changes in the intensities and position of peaks like peaks for amide I, amide II, amide A bands, olefinic band at 3010 cm<sup>-1</sup>, peak at 1401 cm<sup>-1</sup> and 1452 cm<sup>-1</sup> due to methyl group of protein, peaks at 1065 cm<sup>-1</sup> and 1088 cm<sup>-1</sup> etc. The changes in the peak position and intensities were decreased in the spectra of SIB treated group as compared to NDEA-induced group (Figure 11c). Changes in the peak intensities of amide I and amide II bands, reappearance of olefinic band with a shift to 3007 cm<sup>-1</sup>, change in peak near 1720 cm<sup>-1</sup> of ester group, peak near 1024 cm<sup>-1</sup> were observed. The spectra of SIB (50 mg/kg/day) treated group was compared with NDEA-treated group (Figure 11d) were found with variations at numerous peaks such as, amide I and amide II bands, olefinic peak, amide A and B bands, band shift in peaks near 1024 cm<sup>-1</sup>. The FTIR spectra of SIB treated group have similarities with normal control group spectra.

### Discussion

Rats treated with NDEA significantly reduce the body weight might be due to stress compared to control animals. The reduction in body weight of the animals in this study correlate with the decreased food intake observed during the experimental period which appeared to reduced metabolism and hepatotoxicity [38]. Liver damage caused by NDEA and CCl<sub>4</sub> generally reflects instability of liver cell metabolism which leads to distinctive changes in the serum enzyme activities. Serum transaminases, ALP and γ-GT are representative of liver function and their increased levels are indicators of liver damage. The increase in ALT activity is repeatedly credited to hepatocellular damage and is usually accompanied by a rise in AST. Similarly, increase in ALP reflects pathological alteration in biliary flow and discharge of total bilirubin reflects a non-specific alteration in the plasma membrane integrity and/or permeability. γ-GT is an enzyme in the hepatocyte plasma membrane, its liberation into serum indicates cellular damage to liver. Hence γ-GT is considered to be one of the best indicators of liver damage [39]. After partial hepatectomy only a slight to moderate increase in serum transaminase activity was recorded specifically with AST of liver tissue preparation. In patients with hepatocellular carcinoma high preoperative levels of ALT, ALP, AST and γ-GT indicates a significantly increased risk to develop tumor recurrence after

Groups	Group I	Group II	Group III	Group IV	Group V
SOD (U/min/mg protein)	4.87 ± 0.09	4.34 ± 0.078 <sup>a, ns</sup>	2.09 ± 0.068 <sup>a,***</sup>	3.27 ± 0.043 <sup>b,**</sup>	4.03 ± 0.062 <sup>b,***</sup>
CAT (U/min/mg protein)	30.54 ± 0.53	28.61 ± 0.34 <sup>a, ns</sup>	18.37 ± 0.29 <sup>a,***</sup>	23.42 ± 0.54 <sup>b,*</sup>	27.51 ± 0.58 <sup>b,***</sup>
GPx(nmol NADPH oxidized/min/mg protein)	91.2 ± 0.31	85.7 ± 0.31 <sup>a, ns</sup>	58.7 ± 0.46 <sup>a,***</sup>	64.9 ± 1.47 <sup>b,ns</sup>	82.4 ± 0.52 <sup>b,***</sup>
GST(nmol CDNB conjugate/min/mg protein)	387.60 ± 13.64	376.50 ± 11.3 <sup>a, ns</sup>	174.20 ± 11.7 <sup>a,***</sup>	239.5 ± 4.8 <sup>b,**</sup>	368.3 ± 12.7 <sup>b,***</sup>
GSH (nmol GSH/mg tissue)	2.85 ± 0.18	2.23 ± 0.18 <sup>a, ns</sup>	1.21 ± 0.22 <sup>a,***</sup>	1.68 ± 0.46 <sup>b,ns</sup>	2.35 ± 0.21 <sup>b,***</sup>
GR (nmol GR/mg tissue)	3.20 ± 0.44	2.98 ± 0.31 <sup>a, ns</sup>	1.97 ± 0.27 <sup>a,***</sup>	2.61 ± 0.40 <sup>b,**</sup>	3.07 ± 0.53 <sup>b,***</sup>

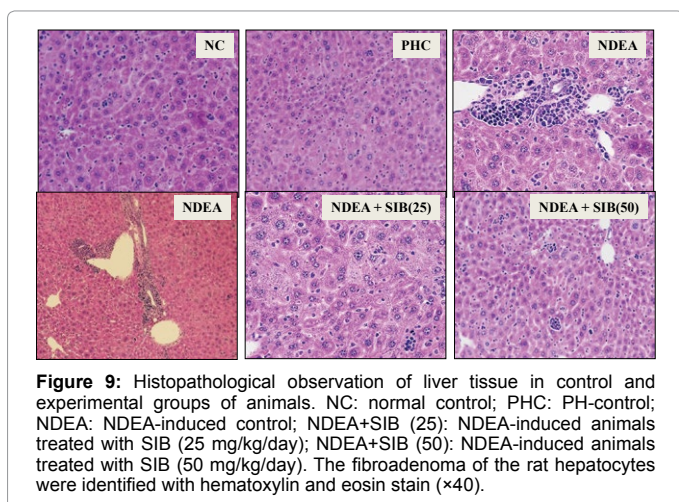
Values are expressed as mean ± SEM for Six animals. Group I: Normal control; Group II: PH-control; Group III: NDEA; Group IV: NDEA+SIB (25 mg/kg/day); Group V: NDEA+SIB (50 mg/kg/day). Comparisons: a = groups II and III with group I; b = group IV and V with group III. Significant: <sup>ns</sup>p>0.05; \*p<0.05; \*\*p<0.01; \*\*\*p<0.001.

**Table 3:** Effect of Silibinin (SIB) on serum antioxidant status of NDEA-induced liver cancer rats.

Groups	Group I	Group II	Group III	Group IV	Group V
SOD(U/mg protein)	8.62 ± 0.32	8.04 ± 0.64 <sup>a, ns</sup>	4.45 ± 0.72 <sup>a,***</sup>	6.36 ± 0.87 <sup>b,**</sup>	8.10 ± 0.49 <sup>b,***</sup>
CAT (U/mg protein)	60.53 ± 1.23	58.23 ± 1.40 <sup>a, ns</sup>	39.26 ± 1.67 <sup>a,***</sup>	47.66 ± 1.5 <sup>b,*</sup>	56.16 ± 1.62 <sup>b,***</sup>
GPx(nmol NADPH oxidized/min/mg protein)	92.45 ± 2.32	89.34 ± 1.24 <sup>a, ns</sup>	43.05 ± 2.21 <sup>a,***</sup>	58.15 ± 1.13 <sup>b,*</sup>	72.34 ± 1.15 <sup>b,***</sup>
GST(nmol CDNB conjugate/min/mg protein)	179.43 ± 2.69	181.45 ± 5.12 <sup>a, ns</sup>	92.82 ± 1.85 <sup>a,***</sup>	129.11 ± 2.32 <sup>b,*</sup>	162.18 ± 3.15 <sup>b,***</sup>
GSH (nmol GSH/mg tissue)	1.52 ± 0.12	1.48 ± 0.14 <sup>a, ns</sup>	0.49 ± 0.09 <sup>a,***</sup>	0.85 ± 0.06 <sup>b,**</sup>	1.43 ± 0.12 <sup>b,***</sup>
Ascorbic acid	8.82 ± 0.13	8.12 ± 0.15 <sup>a,*</sup>	5.23 ± 0.19 <sup>a,***</sup>	6.69 ± 0.13 <sup>b,**</sup>	7.79 ± 0.08 <sup>b,***</sup>
α-Tocopherol	6.14 ± 0.19	5.95 ± 0.25 <sup>a, ns</sup>	3.09 ± 0.12 <sup>a,***</sup>	4.12 ± 0.23 <sup>b,*</sup>	5.85 ± 0.15 <sup>b,***</sup>

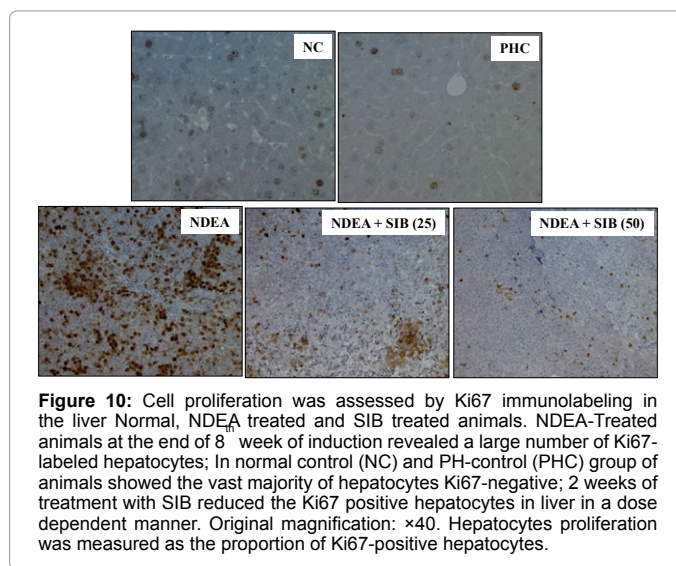
Values are expressed as mean ± SEM for Six animals. Group I: Normal control; Group II: PH-control; Group III: NDEA; Group IV: NDEA+SIB (25 mg/kg/day); Group V: NDEA+SIB (50 mg/kg/day). Comparisons: a = groups II and III with group I; b = group IV and V with group III. Significant: <sup>ns</sup>p>0.05; \*p<0.05; \*\*p<0.01; \*\*\*p<0.001.

**Table 4:** Effect of Silibinin (SIB) treatment on liver oxidative stress indices in homogenate tissue preparation from normal and treatment groups of animals.



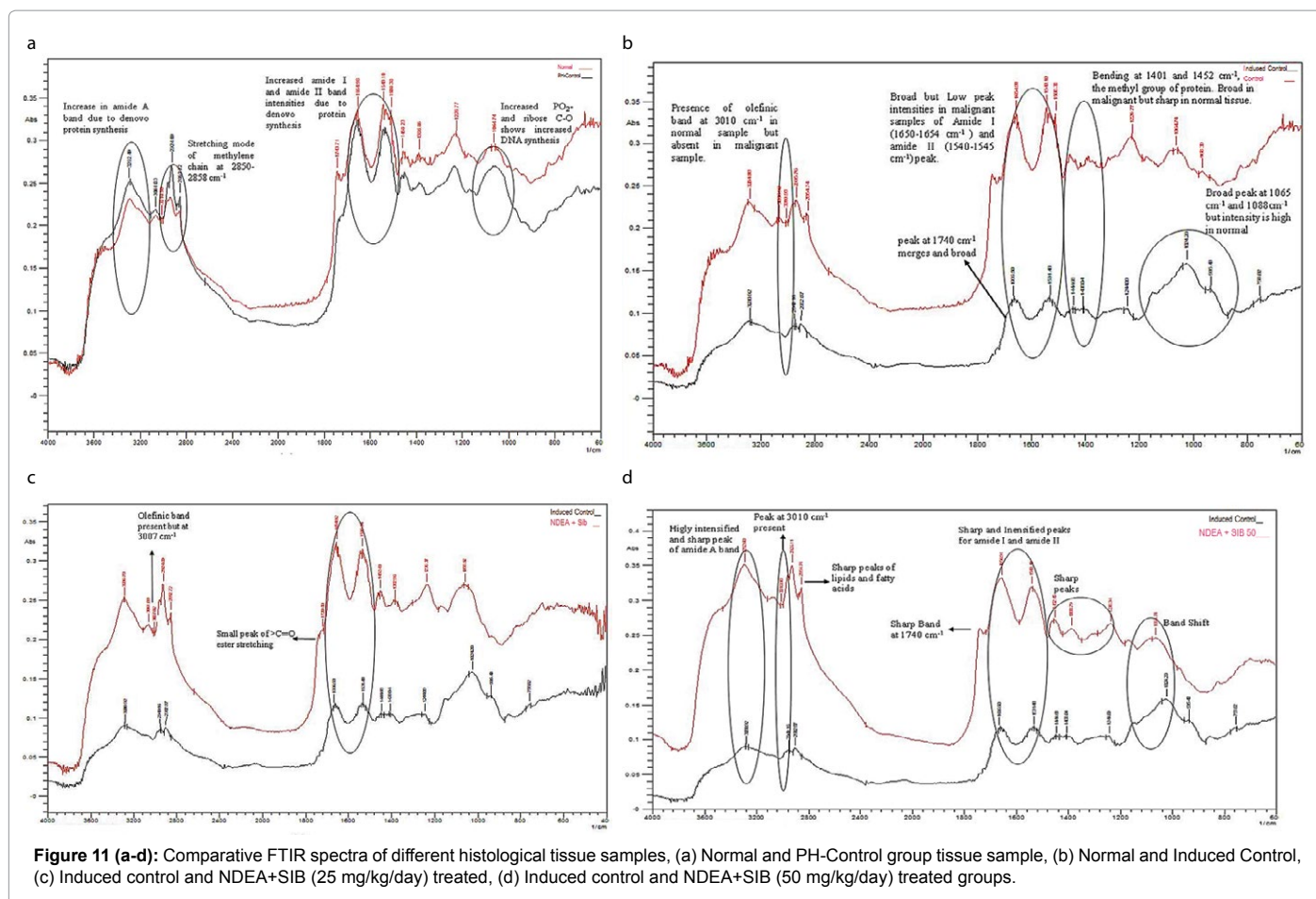
hepatectomy. In the present investigation, in PH control animals, after 8 weeks all enzymes returned to almost normal level (insignificant result with normal control) and also with treatment with SIB lowered the enhanced level of activities of enzymes in HCC animals. It is suggested that SIB tends to prevent liver damage and exhibiting hepatoprotective activity, also aids in parenchyma cell regeneration in liver and thereby protecting membrane integrity by decreased enzyme leakage. This might be the reason for the restoration in the activities of the marker enzymes after administration of SIB for the specified experimental period of treatment.

The results obtained for the level of TC, c-LDL, c-VLDL, TG significantly increased and c-HDL level decreased with NDEA-treatment when compared to control group. Treatment with SIB restores these changes to near normal level. There is always a major changes found in the levels of lipoproteins along with TC and TG with patients with HCC [40]. Liver is the major site involved in the synthesis of sialic acid, hexose and hexosamine glycoproteins. The synthesized glycoproteins are made to circulate in the blood [41]. Sialic acid is an acylated derivative of neuraminic acid and exists



as a terminal component of the non-reducing end of carbohydrate chains of glycoprotein. Their implications in a variety of surface-related vital cell functions in numerous tissues including HCC are well documented. Hence, a pronounced increase in serum levels was recorded. Glycoproteins level was found to be significantly reduced after treatment with SIB (50 mg/kg/day). This study shows that SIB administration may inhibit glycoprotein synthesis in tumor cells [42].

The significant increase of hepatic GSH level in NDEA-treated rat liver is probably due to the simultaneous observed two-fold increase in the activities of γ-GT one of the principal enzymes involved in GSH formation [43]. Glutathione-S-transferases (GSTs) are a family of isoenzymes that play an important role in protecting cells from the cytotoxins and carcinogens. In addition, GSTs can bind to sequester intracellular toxins to prevent oxidative damage by an intrinsic organic peroxidase that converts toxic peroxidase to inactivated form [44]. These results indicate the ameliorative effect of SIB under cancer conditions. Moreover, GSH has a nucleophilic property that makes key



role in the cellular protection from the oxidative damage. Furthermore, GSH is a cofactor of GST, which is responsible for detoxification of xenobiotics. GSH is regenerated by glutathione reductase from the oxidized glutathione. SIB has antioxidant potential which restores these enzymes. Ascorbic acid and  $\alpha$ -tocopherol may also account for its potential anticancer effects. Additionally, we also observed that vitamin C and vitamin E levels were significantly increased in SIB-treated cancer-bearing rats.

Oxidative damage of the vital cellular constituents such as DNA, lipids and proteins and alterations in the signal transduction pathways that control the expression of genes required to execute cell death occurs in the liver tissue due to the formation of large amount of reactive oxygen species. As the present study represented, the increased level of MDA which was a biomarker for the oxidative stress in the liver of HCC bearing animals that could be result to the excessive generation of free radicals which are produced during the metabolism of NDEA or during the process of carcinogenesis [45]. Free radical scavenging activity of SIB is confirmed by the results obtained in our findings i.e. decreased level of MDA after drug treatment. SOD was reported as one of the most important enzymes among the enzymic antioxidant defense system. It scavenges the superoxide anion to form hydrogen peroxide, hence diminishing the toxic effect caused by free radicals. In the present study, the significantly decreased level of SOD as observed in HCC induced animals which might be due to the utilization of the enzyme to scavenge  $H_2O_2$  radicals. CAT decomposes hydrogen peroxide and protects the tissue from highly reactive hydroxyl radicals [46] and it is

thought to be the first line of defense against oxidative damage induced by carcinogen. The significantly decreased level of CAT activities were recorded in NDEA-induced HCC animals as compared to normal animals may be due to the utilization of this enzyme in the removal of hydrogen peroxide radicals caused by carcinogen administration [47]. These antioxidant enzymes have been increased with the treatment of SIB at a dose level of 50mg/kg/day for 2 weeks.

Research reports for cancer diagnosis by infrared spectroscopy have generally focused on some useful findings in molecular level (e.g. amide bands for proteins, symmetric phosphate stretching band of the phosphodiester groups of nucleic acids, methylene chains in membrane lipids, hydrogen bonding on the phosphodiester groups of nucleic acids, methyl to methylene ratio, glycogen content and hydrogen bonding of C—OH groups in carbohydrates and protein etc.) [48]. The vibrational spectra of the protein are characterized by a set of absorption regions known as the amide region and the C-H region. The most widely studied regions are amide I, amide II, amide III and amide A regions. Absorbance at  $1650-1654\text{ cm}^{-1}$  region representing amide I region corresponding to the stretching C=O and bending C—N vibrational modes of the polypeptides and protein backbone and at  $1540-1545\text{ cm}^{-1}$  region assigned to the amide II band corresponding to the bending N—H and stretching C—N [49]. In the amide I band ( $1650-1655$ ) of normal tissues (control group) (Figure 11a) the peak was found to be more intensified than that of NDEA induced cancerous tissue sample. Moreover, the difference between the peak intensity in the NDEA+SIB treated group is significant with respect to induced-

control (Figure 11). The peak shift is insignificant. Uniformity in the peak intensity at 1650-1655  $\text{cm}^{-1}$  was observed in all samples of all the groups. The changes observed are due to the variation and alteration in the protein content and its irregular composition due to alteration in cancer tissue composition and make up of specific vibrational band specially specified for amide I band. The amide I band primarily associates with a stretching motion of the C=O group. This band is sensitive to the environment of the peptide and also depends upon overall secondary structure of protein [50]. The strong band observed at 1659  $\text{cm}^{-1}$  can be assigned to  $\alpha$ -helical structure [51] and amide I band is due to inplane stretching of the C=O bond, weakly coupled with C—N stretching and inplane N—H bending [50]. In the region of amide II band (1540-1545  $\text{cm}^{-1}$ ) the pattern and differences are similar to that of amide I, the peak intensity and position of bands are shifted a little bit due to alteration in protein composition and formation of altered protein in induced group as compared to that of normal control (Figure 11b). The amide II band at about 1550  $\text{cm}^{-1}$  was weak and broad in malignant tissue and was strong and sharp in normal tissue, the NDEA+SIB-50 group also shows the similar peak arrangements as that of observed in normal groups. Further, the Amide A (3200-3300  $\text{cm}^{-1}$ ) band arises due to N—H stretching but is also contributed by O—H stretching and both vibrations represents secondary structure of water soluble proteins [52]. The peak at 3290  $\text{cm}^{-1}$  corresponds to the amide A that can generally be associated with N-H stretching of protein with negligible contribution from O—H stretching of intramolecular hydrogen bonding, since unbound water was removed from the system. Lastly in the amide B the peak at 3078  $\text{cm}^{-1}$  is due to N—H stretching proteins of amide B proteins [37].

The sharp bands of amide I and amide II bands at 1650-1655  $\text{cm}^{-1}$  and 1540-1545  $\text{cm}^{-1}$  respectively are mainly used to indicate the relative concentration of the protein of biological tissues as these bands represents the amide groups of protein. The band at 1401 and 1452 arises mainly from symmetrical and asymmetrical  $\text{CH}_3$  bending modes, respectively of the methyl group of protein [53]. But a broad band is formed in this region (1401-1460  $\text{cm}^{-1}$ ) due to contributions from other bands by different other cellular components like nucleic acids and carbohydrates etc.. The intensity of these bands are higher in normal (Figure 11a) and NDEA+SIB-50 (Figure 11d) treated group than that of malignant tissue (Figure 11b). A significant variation in peak intensity in all the peaks and bands viz. 1260-1290, 1401, 1452, 1540-1545, 1650-1655  $\text{cm}^{-1}$  are observed in the malignant tissue sample. The parameter differs greatly among all treatment group samples on the basis of protein components. Lipid form the major component of cell walls keeping biological media organized in their necessary compartments. In cancer, a very common stage of disease development is called metastasis, which is the complete separation of cancer affected cells, which invade other organs of the body. The main reason for irregular separation of the cells and their easy destruction relates to the quality of their lipid walls, so lipid also plays an important role [54]. The triglycerides contains lots of methyl, methylene and carbonyl, so the different of Fourier transform infrared spectroscopic spectra in normal and malignant tissue at those area were caused by the different contents of lipid substances in the tissue. In the frequency range 3400-2800  $\text{cm}^{-1}$  known as fatty acid region with specific bands at 3300, 3010, 2958, 2925 and 2854  $\text{cm}^{-1}$  corresponding to the stretching mode of OH and/or N—H, H—C=C—H, asymmetrical  $\text{CH}_3$  and both asymmetrical and symmetrical  $\text{CH}_2$  vibrations respectively changes were observed in this fatty acid region while using malignant samples. The band observed at 2920-2925  $\text{cm}^{-1}$  and 2853-2855  $\text{cm}^{-1}$  are due to asymmetric and symmetric stretching modes of the methylene chain in the membrane

lipid respectively [51]. The weak band near 3010/3007  $\text{cm}^{-1}$  in the normal control animal was assigned to the vibration of =CH groups of olefinic bands or unsaturated fatty acids which disappeared in NDEA induced animal tissue sample. A slight shift in the band at 1310  $\text{cm}^{-1}$  was observed in malignant tissue as compared with normal tissue sample. The peak intensities of the band at 2853  $\text{cm}^{-1}$  is higher in normal control group than that of malignant group sample. In malignant tissue sample the intensity of band at 2925  $\text{cm}^{-1}$  was slightly enhanced but with a sharp peak. Taken together, it represents an increase in fatty acid content and/or acryl chain length. The band centered at 1738  $\text{cm}^{-1}$  which was mainly assigned to >C=O ester stretching vibration in phospholipids. An increase in intensity was observed indicating the accumulation of lipid in the NDEA induced group but band is submerged with the peak of amide band due to broadening of the amide bands and increased intensity. Moreover, the intense bands observed at 1466  $\text{cm}^{-1}$  which are due to the  $\text{CH}_2$  asymmetrical bending vibration and  $\text{CH}_3$  symmetrical bending of the lipid. The band intensity was observed to be increased indicating increases in content of fatty acid chains. Further, the band at 1170  $\text{cm}^{-1}$  and 1060  $\text{cm}^{-1}$  which arises due in part of the ester C—O—C asymmetric and symmetric stretching vibrations in phospholipids and cholesterol esters respectively are increased for the malignant tissue and absent in the treatment group of animal tissues, which supports the biochemical finding of our experiment [49]. Major absorption in the spectra of lipid in the control tissue arises from C—C stretching (1117  $\text{cm}^{-1}$ ) and skeletal C—C stretching (1065  $\text{cm}^{-1}$ ) of lipids [53]. DNA and RNA also play important role in relation to protein structures as they carry information that determines protein structure. the main spectral features of nucleic acids in the infrared region are in plane double bond vibrations of the bases, and asymmetric and symmetric phosphate stretching located at 1750-1600  $\text{cm}^{-1}$ , 1230  $\text{cm}^{-1}$  and 1100  $\text{cm}^{-1}$ , respectively. It is also noticeable that the intensity ratio of the signal located at 1055  $\text{cm}^{-1}$  is the most significant difference between DNA and RNA [54]. In NDEA treated tissue sample, nucleic acids gives rise to a medium intensity peak at 1426  $\text{cm}^{-1}$  and a band near 666  $\text{cm}^{-1}$  which are respectively due to the rings breathing modes of DNA bases (alanine, guanine) and ring breathing modes of DNA bases (guanine and thymine) [55]. In malignant tissue the peak at 1220  $\text{cm}^{-1}$  is greater than that of at 1240  $\text{cm}^{-1}$  of the  $\text{PO}_2$  group in phosphodiester group of nucleic acids. In liver cancer many  $\text{PO}_2$  groups of nucleic acids are hydrogen bonded, in contrast to those of normal liver tissue. The band at 1082  $\text{cm}^{-1}$  is mainly due to symmetrical phosphates ( $\text{PO}_2$ ) stretching mode [47]. This band is found higher and stronger in malignant tissue than that in normal tissue. Changes were noted in treated groups and are noticeable which prove the bio-structural changes due to malignancy and are brought back to almost normal levels after the Silibinin treatment. Our work defines, SIB could be a useful and novel therapeutic drug to control HCC. Further preclinical and clinical trials are warranted to research the full potential of this important natural flavonoid analogue.

#### Acknowledgements

Authors need to express thanks to All India Council of Technical Education for the Fellowship support. Authors are greatly acknowledge the authorities of Birla Institute of Technology for the necessary facilities provided for the smooth running of the project and also, thankful to Department of Health, Medical Education and Family welfare, Government of Jharkhand for the continuous encouragement and support towards biomedical research.

We declare no conflict of interest.

#### Author contributions

SP Pattanayak and A Kumar performed the majority of the experiments.

P Sunita performed some histological staining procedure. P Sunita and SP Pattanayak designed the experiments and wrote the manuscript. All authors discussed the results and commented on the manuscript.

## References

1. Qian Y, Ling CQ (2004) Preventive effect of Ganfujian granule on experimental hepatocarcinoma in rats. *World J Gastro* 10: 755-757.
2. Parkin DM, Bray F, Ferlay J, Pisani P (2002) Global cancer statistics. *CA Can J Clin* 55: 74-108.
3. Farazi PA, DePinho RA (2006) Hepatocellular carcinoma pathogenesis: from genes to environment. *Nat Rev Can* 6: 674-687.
4. Brown JL (1999) N-Nitrosamines. *Occup Med* 14: 839-848.
5. Yadav AS, Bhatnagar D (2007) Chemopreventive effect of Star anise in N-nitrosodiethylamine initiated and phenobarbital promoted hepatocarcinogenesis. *Chem Biol Interact* 169: 207-214.
6. Sengupta A, Ghosh S, Das S (2004) Modulatory influence of garlic and tomato on cyclooxygenase-2 activity, cell proliferation and apoptosis during azoxymethane induced colon carcinogenesis in rat. *Can Lett* 208: 127-136.
7. Deml E, Schwarz LR, Oesterle D (1993) Initiation of enzyme-altered foci by the synthetic steroid cyproterone acetate in rat liver foci bioassay. *Carcinogenesis* 14: 1229-1231.
8. Pound AW, Lawton TA, Horn L (1973) Increased carcinogenic action of dimethylnitrosamine after prior administration of carbon tetrachloride. *Br J Expt Path* 27: 451-459.
9. Harborne JB, Williams CA (2000) Advances in flavonoid research since 1992. *Phytochem* 55: 481-504.
10. Ramasamy K, Agarwal V (2008) Multitargeted therapy of cancer by Silymarin. *Can Lett* 269: 352-362.
11. Chen C, Huang T, Wong C, Hong C, Tsai Y, et al. (2009) Synergistic anti-cancer effect of baicalin and silymarin on human hepatoma HepG2 Cells. *Food Chem Tox* 47: 638-644.
12. Hoofnagle JH (2005) Milk thistle and chronic liver disease. *Hepato* 42: 4.
13. Kaur M, Agarwal R (2007) Silymarin and epithelial cancer chemoprevention: How close we are to bedside? *Tox App Pharm* 224: 350-359.
14. Narayana KR, Reddy MS, Chaluvadi MR, Krishna DR (2001) Bioflavonoids classification, pharmacological, biochemical effects and therapeutical potential. *Ind J Pharm* 33: 2-16.
15. Negi AS, Kumar JK, Luqman S, Shanker K, Gupta MM, et al. (2008) Recent advances in plant hepatoprotectives: a chemical and biological profile of some important leads. *Med Res Rev* 28: 746-772.
16. Cheung CW, Vesey DA, Nicol DL, Johnson DW (2007) Silibinin inhibits renal cell carcinoma via mechanisms that are independent of insulin-like growth factor-binding protein 3. *BJU Int* 99: 454-460.
17. Zhang S, Yang Y, Liang Z, Duan W, Yang J, et al. (2013) Silybin-mediated inhibition of Notch signaling exerts antitumor activity in human hepatocellular carcinoma cells. *PLoS One* 8: e83699.
18. Bousserouel S, Bour G, Kauntz H, Gossé F, Marescaux J, et al. (2012) Silibinin inhibits tumor growth in a murine orthotopic hepatocarcinoma model and activates the TRAIL apoptotic signaling pathway. *Anticancer Res* 32: 2455-2462.
19. King J (1965) The alanine transaminase and aspartate transaminase. In: Van D (ed) *Practical clinical enzymology*. Nostrand, London p. 121-138.
20. Pattanayak SP, Mazumder PM (2010) Therapeutic potential of *Dendrophthoe falcata* (L.f.) Ettingsh on 7,12-dimethyl benz(a)anthracene-induced mammary tumorigenesis in female rats: effect on antioxidant system, lipid peroxidation and hepatic marker enzymes. *Comp Clin Pathol* 20: 381-392.
21. Belfield A, Goldberg D (1971) Colorimetric determination of alkaline phosphatase activity. *J Clin Path* 12: 561-566.
22. Szasz G (1969) Kinetic determination of serum gamma glutamyl transferase. *Clin Chem* 15: 124-126.
23. Ohkawa H, Ohishi N, Yagi K (1979) Assay of lipid peroxides in animal tissues by thiobarbituric acid reaction. *Anal Biochem* 95: 351-358.
24. Lowry OH, Rosebrough NJ, Farr AL, Randall RJ (1951) Protein measurement with the Folin-phenol reagent. *J Biol Chem* 193: 265-275.
25. Flohe L, Otting F (1984) Superoxide dismutase assays. *Meth Enzymol* 105: 93.
26. Sinha AK (1972) Colorimetric assay of catalase. *Anal Biochem* 47: 389-394.
27. Rotruck JT, Pope AL, Ganther HE, Swanson AB, Hafeman DG, et al. (1973) Selenium: biochemical role as a component of glutathione peroxidase. *Science* 179: 588-590.
28. Habig WH, Pabst MJ, Jakoby WB (1974) Glutathione-S-transferase: the first enzymatic step in mercapturic acid formation. *J Biol Chem* 249: 7130-7139.
29. Folch J, Less M, Stanely GHS (1951) A simple method for the isolation and purification of total lipids from animal tissues. *J Biol Chem* 226: 504-509.
30. Rice EW (1970) Triglycerides in serum. In: Roderick P, Mac-Donald CH (eds) *Standard methods of clinical chemistry*, 6th edn. Academic Press, New York, pp 215-222.
31. Van Handle E (1961) Modification of the micro determination of triglycerides. *Clin Chem* 7:249-251.
32. Parkeh AC, Jung DH (1970) Cholesterol determination with ferric chloride uranium acetate and sulphuric acid-ferrous sulphate reagents. *Anal Chem* 42: 1423-1427.
33. Sujatha V, Sachdanandam P (1997) Effect of *Semicarpus anacardium* Linn nut extract on experimental mammary carcinoma in Spague- Dawley rats with reference to tumor marker enzymes. *Pharm Pharmacol Commun* 6: 375-379.
34. Nandave M, Ojha S K, Kaur R (2005) Changes in levels of serum glycoproteins in major depressive disorders. *Indian J Clin Biochem* 20: 154-157.
35. Pattanayak S P, Sunita P, Mitra Mazumder P (2014) Restorative effect of *Dendrophthoe falcata* (L.f.) Ettingsh on lipids, lipoproteins, and lipid-metabolizing enzymes in DMBA-induced mammary gland carcinogenesis in Wistar female rats. *Comp Clin Pathol* 23:1013-1022.
36. Rosmorduc O, Wendum D, Corpechot C, Galy B, Sebbagh N, et al. (1999) Hepatocellular hypoxia-induced vascular endothelial growth factor expression and angiogenesis in experimental biliary cirrhosis. *Am J Pathol* 155: 1065-1073.
37. Palaniappan PR, Vijaysundaram V, Prabu SM (2011) A study of the subchronic effects of Arsenic exposure on the liver tissue of Lebeo Rohita using Fourier transform infrared technique. *Environ Toxicol* 26: 338-344.
38. Lee SJ, Boyer TD (1993) The effect of hepatic regeneration on the expression of the glutathione-S-transferases. *Biochem J* 293: 137-142.
39. Singh BN, Singh BR, Sharma BK, Singh HB (2009) Potential Chemoprevention of N-nitrosodiethylamine-induced hepatocarcinogenesis by polyphenolics from *Acacia nilotica* bark. *Chem Biol Int* 181: 20-28.
40. Cooper ME, Hardy KJ (1996) Effects of liver transplantation and resection on lipid parameters: a longitudinal study New Zealand. *J Surgery* 66: 743-746.
41. Weiden S (1958) Serum Hexosamine levels in health and disease. *J Clin Pathol* 11: 177-182.
42. Klaunig JE, Kamendulis LM (2004) The role of oxidative stress in carcinogenesis. *Ann Rev Pharm Tox* 44: 239-267.
43. Sukata T, Uwagawa S, Ozaki K, Sumida K, Kikuchi K, et al. (2004) Alpha(2) Macroglobulin: a novel cytochemical marker characterizing preneoplastic and neoplastic rat liver lesions negative for hitherto established cytochemical markers. *Am J Pathol* 165: 1479-1488.
44. Valderrama B, Ayala M, Vazquez-Duhalt R (2002) Suicide inactivation of peroxidases and the challenge of engineering more robust enzymes. *Chem Biol* 9: 555-565.
45. Sundaresan S, Subramanian S (2003) S-allylcysteine inhibits circulatory lipid peroxides and promotes in N-nitrosodiethylamine induced carcinogenesis. *Pol J Pharm* 55: 37-42.
46. Dakshayani KB, Subramanian P, Manivasagam T, Essa M, Manoharan S (2005) Melatonin modulates the oxidant-antioxidant imbalance during N-Nitrosodiethylamine induced Hepatocarcinogenesis. *J Pharm Sci* 8: 316-321.
47. Wong PTT, Wong RK, Caputo TA, Goodwin TA, Rigas B(1991) Infrared spectroscopy of exfoliated human cervical cells: Evidences of extensive structural changes during carcinogenesis. *Proc Nat Acad Sci* 88: 10988-10992.
48. Melin AM, Perromat A, Deleris G (1999) Pharmacologic application of fourier

- transform IR spectroscopy: In vivo toxicity of carbon tetrachloride on Rat liver. *Biopol Biospectro* 57: 160-168.
49. Venkataramana GV, Kumar JK, Devi Prasad AG, Karimi P (2010) Fourier transform infrared spectroscopy study on liver of Freshwater Fish *Oreochromis Mossambicus*. *Rom J Biophy* 20: 315-322.
50. Damania G, Cavalu S, Miclaus V, Sabau L, Vedeanu N, et al. (2007) EPR and ATR-FTIR investigation of lyophilized cytochrome C at different pH. *Rom J Biophy* 17: 139-148.
51. Yang Y, Sule-Suso J, Sockalingum GD, Kegelaer G, Manfait M, et al. (2005) Study of tumor cell invasion by Fourier transform infrared microspectroscopy. *Biopoly* 78: 311-317.
52. Eckel R, Huo H, Guan HW, Hu X, Che X, et al. (2001) Characteristic infrared spectroscopic patterns in the protein bands of human breast cancer tissue. *Vib Spectro* 27: 165-173.
53. Movasaghi Z, Rehman S, Rehman IU (2008) Fourier transform infrared Spectroscopy of biological tissues. *Appl Spectro Rev* 43: 134-179.
54. Krishnakumar N, Manoharan S, Palaniappan PLRM, Venkatachalam P, Arun manohar MG (2009) Chemopreventive efficacy of Piperine in 7,12-dimethyl benz[a] anthracene(DMBA)-induced hamster buccal pouch carcinogenesis: An FT-IR study. *Food chem Techno* 23: 45-51.
55. Wang JS, Shi JS, Xu YZ, Duan XY, Zhang L, et al. (2003) FT-IR spectroscopic analysis of normal and cancerous tissues of esophagus. *World J Gastro* 9: 1897-1899.